

Title No. 114-S58

Effect of Combining Near-Surface-Mounted and U-Wrap Fiber-Reinforced Polymer Strengthening Techniques on Behavior of Reinforced Concrete Beams

by Rahulreddy Chennareddy and Mahmoud M. Reda Taha

Flexural strengthening of reinforced concrete (RC) beams using near-surface-mounted (NSM) fiber-reinforced polymers (FRP) and U-wrap FRP shear strengthening are two well-established methods. There is a fair chance that the two aforementioned techniques might be mixed in strengthening of RC beams. This research examines the behavior of RC beams strengthened using NSM and U-wrap FRP strengthening. The NSM-FRP flexural strengthening technique is strongly dependent on the performance of bond between the NSM-FRP bar and the surrounding epoxy. Tension rupture of the NSM-FRP bar is highly unlikely, even when a full development length is provided. However, when U-wrap FRP is considered, confinement has shown to improve the bond strength of NSM-FRP bars and marginally increase the flexural capacity of strengthened RC beams. However, the improvement in the bond strength of NSM-FRP bars results in changing the NSM-FRP debonding to an abrupt failure caused by NSM-FRP bar rupture. Special care should be taken in designing RC strengthening combining NSM and U-wrap FRP strengthening.

Keywords: ductility; fiber-reinforced polymers (FRPs); near surface mounting (NSM); U-wrap shear strengthening.

INTRODUCTION

Recent statistics by the Federal Highway Administration (FHWA) have shown that 24% of the bridges in the United States are structurally deficient.¹ This deficiency is strongly related to the low durability of reinforced concrete (RC) elements² and necessitates strengthening to reach desired performance. Fiber-reinforced polymers (FRP) have made attractive alternative materials for strengthening RC structures.³

Typically, flexural strengthening of RC beams using FRP is performed in one of two configurations: externally bonded (EB) FRP and near-surface-mounted (NSM)-FRP. In EB-FRP, an FRP laminate is bonded to the tension face of the beam using epoxy polymer to allow the FRP laminate to act as an additional reinforcement contributing to the overall flexural capacity of the beam.⁴ With NSM-FRP, a saw-cut groove is made on the tension face of the beam, the groove is half-filled with epoxy, and additional FRP reinforcement is placed in this groove. The groove is then completely filled with epoxy and left to cure.⁵ The NSM-FRP flexural strengthening technique enables better bond compared with EB-FRP and hence many designers prefer NSM-FRP to EB-FRP.^{6,7}

The possible failure modes for RC beams strengthened with NSM-FRP technique include FRP-rupture or debonding of NSM FRP after yield of the tension steel.⁶ Bond is a critical issue for efficient performance of the NSM-FRP technique. Although a full bond development length is provided

for the NSM-FRP bar, Hassan and Rizkalla⁷ showed that it is highly unlikely that FRP rupture will occur. This is attributed to the fact that, typically, the FRP bar will experience only 60 to 70% of the ultimate tensile capacity of FRP. The bond performance of NSM-FRP was examined in two configurations: direct pullout test^{6,8,9} and beam pullout flexure test.^{7,10} A comprehensive experimental and computational investigation was performed to understand the stress transfer between the epoxy-FRP interface and the epoxy-concrete interface for different groove sizes, thereby developing design charts for NSM-FRP.⁷ A detailed review of all possible modes of debonding can be found elsewhere.⁶ As debonding is the main mode of failure, the flexural capacity is predicted by estimating tensile strain capacity of the FRP bar using principles of strain compatibility.¹¹ It was demonstrated that FRP debonding is the governing failure mode for NSM-FRP strengthened RC-beams.⁷

The following Eq. (1) and Eq. (2) have been used to estimate the ultimate capacity of the FRP strengthened RC beams based on ACI 440.2R-08.¹¹

$$C = \frac{A_s \cdot f_y + A_f \cdot f_{fe} - A'_s \cdot E_y \cdot \epsilon'_s}{0.85 f'_c B \beta_1} \quad (1)$$

where C is the depth of compression zone from force equilibrium; A_s is the area of tension steel used for reinforcement; f_y is the yield stress of tension steel; A_f is the area of FRP in tension used for reinforcement; f_{fe} is the effective stress in FRP after considering the debonding strain of NSM-FRP; A'_s is the area of steel used for compression reinforcement; E_y is the modulus of elasticity of steel; ϵ'_s is the strain in compression steel ≤ 0.0021 ; f'_c is 28 days compressive strength of concrete; B is the width of the beam; and β_1 is the concrete stress block coefficient.

$$M_n = A_s f_y \left(d_s - \frac{a}{2} \right) + \psi_f A_f f_{fe} \left(d_f - \frac{a}{2} \right) - A'_s f_y \left(d'_s - \frac{a}{2} \right) \quad (2)$$

where M_n is the nominal moment capacity of the RC beam; d_s is the distance between centerline of the steel rebar to

ACI Structural Journal, V. 114, No. 3, May-June 2017.

MS No. S-2015-441.R2, doi: 10.14359/51689443, was received August 13, 2016, and reviewed under Institute publication policies. Copyright © 2017, American Concrete Institute. All rights reserved, including the making of copies unless permission is obtained from the copyright proprietors. Pertinent discussion including author's closure, if any, will be published ten months from this journal's date if the discussion is received within four months of the paper's print publication.

top of the concrete; a is the depth of Whitney's compression block; ψ_f is the FRP strength reduction factor; d_f is the distance between the centerline of the NSM-FRP reinforcing bar to the top of the concrete; and d_s' is the distance between the centerline of the compression steel reinforcing bar to the top of the concrete.

U-wrap using FRP is a well-known shear strengthening technique. U-wrap FRP uses the wet layup technique, in which the FRP fabric is saturated in epoxy, and this saturated FRP fabric is adhered to the concrete surface of the flexural member with orientation of the fibers in the desired shear reinforcement direction. FRP shear strengthening has been adopted in three configurations: completely wrapped, three-sided U-wrap, and two-sided¹¹ FRP. The significance of the wrapping scheme on the efficiency of shear strengthening of existing beams and columns was widely investigated.¹²⁻¹⁴ The effect of U-wrap FRP on the flexural behavior of NSM steel has been investigated and showed a significant improvement in the flexural capacity for the combined strengthened beams avoiding a premature failure of the RC beams strengthened with NSM steel only.¹⁵

In practical field applications, NSM-FRP for flexural strengthening and U-wrap for shear strengthening were combined to meet flexural and shear demands of RC beams. Nevertheless, the effect of combining U-wrap shear strengthening and NSM-FRP flexural strengthening techniques has never been reported. ACI 440.2R-08¹¹ treats the two techniques separately and thus a designer might consider the two techniques to be independent and their effect to be additive. The objective of this study is to examine the significance of U-wrap shear strengthening on the bond performance and thus the flexural behavior of NSM-FRP-strengthened RC beams. The hypothesis is that U-wrapping will provide confinement to the NSM-FRP reinforcement and thus will improve the bond strength of FRP to epoxy. This improvement might be significant to prevent the typical debonding of FRP and thus might change the mode of failure to FRP rupture causing a sudden and abrupt failure of RC beam specimens.

Three main approaches were used in the current study to quantify deformability of NSM-FRP-strengthened RC beams; energy model proposed by Naaman and Jeong¹⁶; moment and deformation model proposed by Jaeger et al.¹⁷ and Zou¹⁸; and deflection-based model proposed by Abdelrahman et al.¹⁹

The energy model by Naaman and Jeong¹⁶ is mainly based on the ratio between total energy and elastic energy released at failure under a load-versus-deflection curve or a moment-curvature curve. The ductility index was calculated based on moment-curvature curve. For the current study, elastic energy was calculated based on the slope of the moment-curvature curves as suggested by Naaman and Jeong.¹⁶ The ductility index is given by

$$\mu = 0.5 \left(\frac{E_{tot}}{E_{el}} + 1 \right) \quad (3)$$

where μ is the ductility index; E_{tot} is the total area under the moment-curvature curve; and E_{el} is the elastic energy or

the area under the anticipated linear elastic part of the load deflection curve.

Jaeger¹⁷ suggested the deformability index based on the moment-curvature relationship as described by Eq. (4).

$$J = \frac{\phi_u M_u}{\phi_{SE} M_{SE}} \quad (4)$$

where ϕ_u and ϕ_{SE} are the curvatures of flexural members at ultimate and service moments M_u and M_{SE} , respectively. In the current study, the service moment is the moment corresponding to a 0.001 strain in the top concrete compression fibers. The aforementioned method is recommended for ensuring deformability prior to failure of concrete elements reinforced with FRP and undergoing tension failure.¹⁷

Abdelrahman et al.¹⁹ proposed a model based on the ratio of deflection corresponding to the ultimate load with the cracked stiffness (Δ_2) to the deflection corresponding to ultimate load with uncracked stiffness (Δ_1), as described by Eq. (5)

$$\mu = \frac{\Delta_2}{\Delta_1} \quad (5)$$

RESEARCH SIGNIFICANCE

During the last decade, NSM-FRP became a widely accepted field technique for flexural strengthening of RC beams. Combining flexural and shear strengthening of RC beams using FRP is a common practice. Such combination is allowed by ACI guidelines to strengthen RC beams using FRP as two independent strengthening methods. However, shear strengthening using U-wrap FRP sheets might influence the bond-slip behavior of NSM-FRP and thus might change the mode of failure and affect the ductility of the strengthened RC-beams. This research examines this combined effect and suggests provisions to be considered by design guidelines.

EXPERIMENTAL METHODS

A test matrix of 25 beams, classified to a set of five RC beams per type, was tested under static loading to failure under four-point bending configuration. Five RC beams with only steel as reinforcement were designated as "C" followed by its number (C1 through C5). Five RC beams with steel as reinforcement were strengthened for shear using the three-sided FRP U-wrap technique designated as "U" followed by the corresponding beam number (U1 through U5). The significance of this RC beam series was to check if the U-wrap shear strengthening made any contribution toward the flexural capacity of the strengthened RC members. Five RC beams with steel as reinforcement were flexurally strengthened using the NSM-FRP technique only designated as "N" followed by the corresponding beam number (N1 through N5). This group worked as a reference to demonstrate the behavior of NSM-FRP-strengthened RC beams. Five RC beams with steel as reinforcement were flexurally strengthened using the NSM-FRP technique and also shear strengthened using U-wrap along the whole beam span designated as "NU" followed by the corresponding beam

Table 1—Material properties

Material	Modulus of elasticity, MPa (ksi)	Tensile yield strength, MPa (ksi)	Ultimate tensile strength, MPa (ksi)	Elongation at break, %	Compressive strength, MPa (ksi)
Concrete at 28 days	41,335 (6000)	—	—	—	55 (8)
Steel reinforcing bar	200,000 (29,000)	414 (60)	620 (90)	—	620 (90)
GFRP reinforcing bar	46,000 (6600)	—	827 (120)	1.79	—
Dural LPL MV at 14 days	1172 (170)	—	21 (3)	—	69 (10)

number (NU1 through NU5). This group was used to investigate the effect of U-wrap shear strengthening on NSM-FRP flexurally strengthened RC beams. Finally, five RC beams with steel as reinforcement were flexurally strengthened using the NSM-FRP technique and also shear strengthened using U-wrap shear strengthening, where the wrap was used only in the shear area. This group was designated as “NUS” followed by the corresponding beam number (NUS1 through NUS5). The significance of this group was to investigate the effect of limited U-wrap shear strengthening.

The 25 RC beam dimensions were 152 mm wide x 152 mm deep x 763 mm long (6 in. x 6 in. x 30 in.). All RC beams were reinforced with two No. 3 (nominal diameter 10 mm) steel reinforcing bar as tension and compression reinforcement. All the beams were shear reinforced with No. 3 closed stirrups spaced at 76 mm (3 in.) center to center. The clear cover for the tension and compression side was 55.8 mm (2.2 in.) and 29.5 mm (1.2 in.), respectively. The material properties of the concrete and No. 3 (nominal diameter 10 mm [3/8 in.]) steel reinforcing bar are summarized in Table 1. Figure 1 presents the dimensions and details of the RC beams used in the current study. Figure 2 presents all the RC beam series tested in this study.

The beam series “N,” “NU,” and “NUS” strengthened with NSM-FRP flexural strengthening were cast with a precast groove for NSM onto the tension soffit with 25.4 mm wide x 25.4 mm deep (1 in. x 1 in.). After the beams were cured for 28 days, the beams series “N,” “NU,” and “NUS” were strengthened using the NSM-FRP flexural strengthening technique using glass FRP (GFRP) No. 3 reinforcing bar (nominal diameter 10 mm [3/8 in.]). With the precast groove already present, the ends of the groove were sealed with a silicon sealant while the GFRP bar was supported at a desired height such that the GFRP bar was exactly placed at the center of the groove, then the groove was filled with epoxy and allowed to cure. GFRP spirally wound with sand-coated reinforcing bar was used for NSM-FRP strengthening because of the efficient bond performance of those bars and their availability.²⁰ The mechanical properties of the GFRP reinforcing bar are summarized in Table 1. Epoxy was used for the NSM flexural strengthening technique. The mechanical properties of this epoxy are summarized in Table 1.

The beam series “U,” “NU,” and “NUS” were shear strengthened using U-wrap shear strengthening. For the beam series “NU” and “NUS”, the U-wrap technique was performed after flexural strengthening using the NSM-FRP technique was carried out. A U-wrap shear strengthening technique was performed using the wet layup technique. The U-wrap technique requires careful surface preparation of the beams to ensure high surface roughness without air

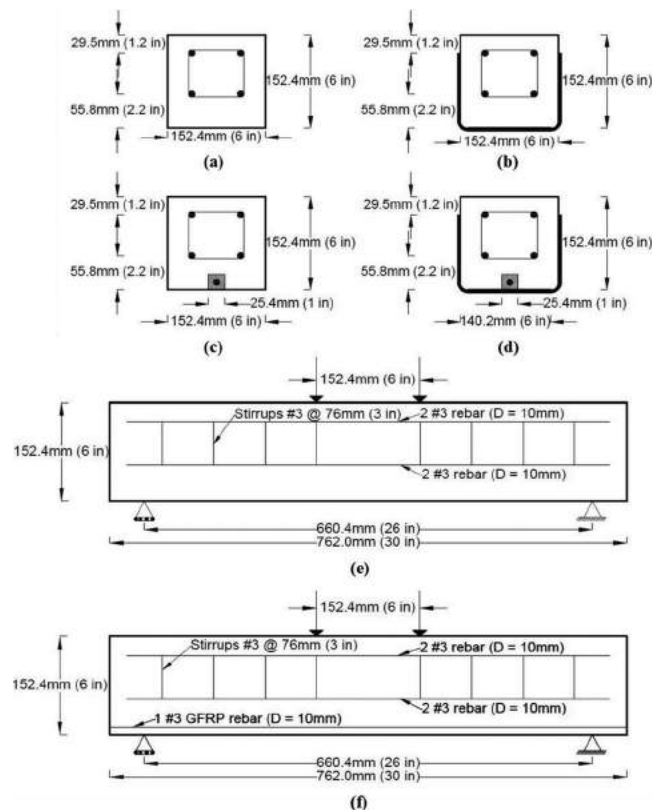


Fig. 1—Cross section of all RC beams series: (a) RC beam control ‘C’; (b) beam with U-wrap only ‘U’; (c) beam with NSM only ‘N’; (d) beam with NSM and U-wrap ‘NU’ and beam with NSM and U-wrap in shear zone only ‘NUS’; (e) longitudinal section corresponding to beam series C and U; and (f) longitudinal section corresponding to beam series N, NU, and NUS.

pockets and no sharp edges. This preparation is necessary to enhance bond performance and avoid premature debonding failure. An angle concrete grinder was used in this study for surface grinding and for rounding the sharp edges prior to application of FRP. A glass fiber composite system was used for U-wrap shear strengthening. This epoxy, a two-component epoxy system, and 1 mm (0.04 in.) thick unidirectional glass-fiber fabric were used. GFRP laminate properties included an ultimate tensile strength in the primary fiber direction of 575 MPa (83 ksi), failure strain of 2.2%, tensile modulus of elasticity 26.1 GPa (3800 ksi), and a nominal laminate thickness of 1.3 mm (0.05 in.).

All of the 25 RC beams were tested under static load to failure using a four-point bending configuration as shown in Fig. 3. The beams were loaded under displacement control of 1 mm/min (0.04 in./min) up to a deflection of

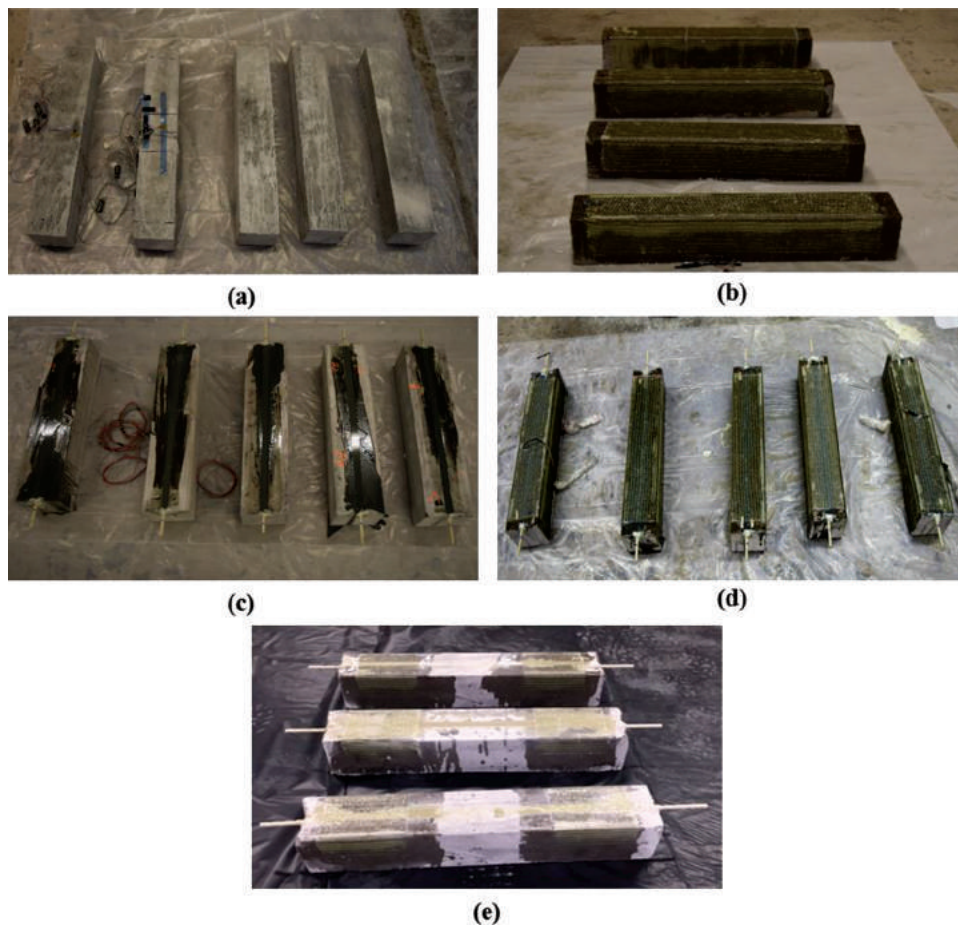


Fig. 2—RC beams ready for testing: (a) simple RC beam control ‘C’; (b) shear strengthened using U Wrap ‘U’; (c) flexural strengthened with NSM FRP ‘N’; (d) NSM FRP flexural and complete U-wrap shear-strengthened beams ‘NU’; and (e) NSM FRP flexural and U-wrap shear strengthened only in shear area ‘NUS’. (Note: Span of beam is 762 mm [30 in].)

15 mm (0.59 in.), and the rate was increased to 3 mm/min (0.12 in./min) up to failure. The two concentrated loads were spaced at 152 mm (6.00 in.) at the midspan of the beam. The distance between the two supports was 660 mm (26.00 in.) with one support pinned and the other support acting as a roller. Testing was carried out on a loading frame connected to a controller data acquisition system. The system recorded loads and cross-head displacements at 1 Hz. Linear variable differential transducers (LVDTs) were placed at the end face on each side of the beam to measure slip of the NSM GFRP bar. Strain gauges were used to measure the strain in top compression fibers, compression steel, tension steel, and GFRP bar.

RESULTS AND DISCUSSION

The experimental results of all the beams tested experimentally are presented in Table 2. A load deflection of the median beam from each series is also shown in Fig. 4. For the control RC beams C1 through C5, the mean ultimate load at failure is $67.3 \text{ kN} \pm 4.0 \text{ kN}$ (15.1 kip \pm 0.9 kip) and the corresponding mean deflection is $10.6 \text{ mm} \pm 0.6 \text{ mm}$ (0.4 in. \pm 0.02 in.). The load-deflection behavior of the “C” series shows a typical RC beam behavior, where the load is linear elastic up to 52.3 kN (11.7 kip) and then a nonlinear behavior can be observed up to the failure load. For RC beams U1 through U5 with a three-sided GFRP U-wrap, the mean ulti-

mate load at failure is $72.1 \text{ kN} \pm 1.7 \text{ kN}$ (16.20 kip \pm 0.38 kip) and the corresponding mean deflection is $10.6 \text{ mm} \pm 1.9 \text{ mm}$ (0.42 in. \pm 0.07 in.). The load-deflection behavior of the “U” series is a typical RC beam behavior, where the load deflection curve is linear elastic up to a mean load of 52.7 kN (11.9 kip) and then a nonlinear behavior is observed up to the failure load. The difference in ultimate strength is insignificant. For RC beams N1 through N5 with NSM-FRP, the mean ultimate load at failure is $98.9 \text{ kN} \pm 2.9 \text{ kN}$ (22.2 kip \pm 0.65 kip) with a corresponding mean deflection of $9.9 \text{ mm} \pm 1.4 \text{ mm}$ (0.39 in. \pm 0.05 in.). The load-deflection behavior of the “N” series is different from the control “C” beams and “U” series. The load-deflection curve is linearly elastic up to a mean load of 69.1 kN (15.5 kip) and then a change in slope is observed where the behavior continues to be linear up to the peak load. Nonlinearity then appears and the load drops relatively slowly as the GFRP slip takes place until failure takes place. For RC beams NU1 through NU5 strengthened with NSM-FRP bars and U-wrap shear strengthening for the full span, the mean ultimate load at failure is $119.1 \text{ kN} \pm 2.6 \text{ kN}$ (26.8 kip \pm 0.6 kip) with a corresponding mean deflection of $14.2 \text{ mm} \pm 2.2 \text{ mm}$ (0.56 in. \pm 0.09 in.). The load-deflection behavior is similar to the “N” series up to a load similar to the peak load of the “N” series. However, the load continues to slightly increase and does not drop. No slip takes place and failure happens abruptly with sudden

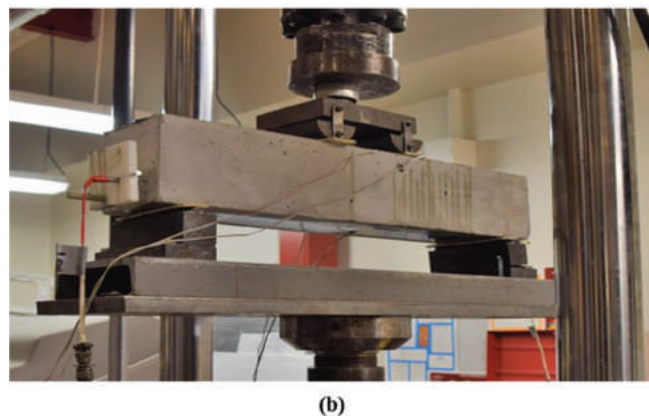
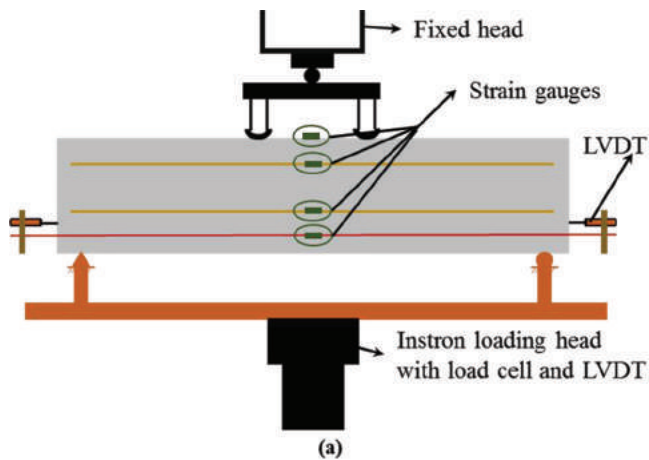


Fig. 3—Four-point bending configuration: (a) schematic showing experimental and instrumentation; (b) snapshot of experimental setup showing LVDT to ends to measure end slip of GFRP bar.

loss of capacity. Rupture of the GFRP bars is evident for the “NU” series. For RC beams NUS1 through NUS5 strengthened with NSM-FRP flexural strengthening and U-wrap for the shear span, the mean ultimate load at failure is $111.8 \text{ kN} \pm 4 \text{ kN}$ ($25.1 \text{ kip} \pm 0.9 \text{ kip}$) versus a corresponding mean deflection of $16.7 \text{ mm} \pm 3.3 \text{ mm}$ ($0.66 \text{ in.} \pm 0.13 \text{ in.}$). The load-deflection behavior of the “NUS” is very similar to that of the “N” series, except that the mode of failure is different where a combined tension rupture of GFRP and/or split of epoxy is observed.

The load-deflection behavior shown in Fig. 4 makes it evident that the behavior is significantly affected when NSM-FRP flexural and U-wrap shear strengthening are combined. The U-wrap significantly increases the load-carrying capacity of the RC beams by 20% for full span U-wrap and by 13% for shear span U-wrap compared with NSM-FRP flexural

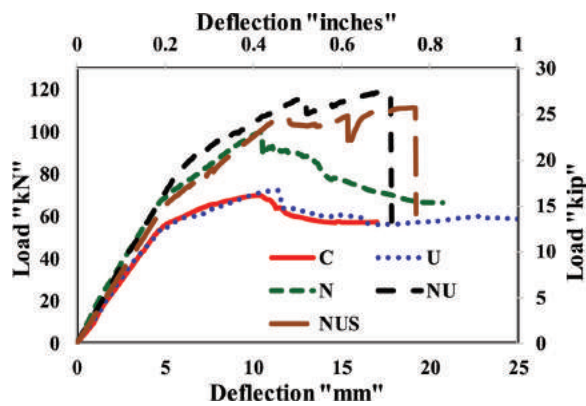


Fig. 4—Load-deflection behavior of median RC beams from all testing series.

Table 2—Results of experimental program at ultimate

Beam type		C1	C2	C3	C4	C5	Mean
Control	Load, kN (kip)	65.4 (14.7)	62.9 (14.1)	65.3 (14.7)	70.2 (15.8)	72.6 (16.3)	67.3 (15.1)
	Deflection, mm (in.)	10.9 (0.4)	10.1 (0.4)	11.4 (0.4)	10.3 (0.4)	10.2 (0.4)	10.6 (0.4)
	Failure mode	CC	CC	CC	CC	CC	—
Beam Type		U1	U2	U3	U4	U5	—
U-wrap only	Load, kN (kip)	73.0 (16.4)	72.7 (16.3)	72.5 (16.3)	73.3 (16.5)	69.2 (15.6)	72.1 (16.2)
	Deflection, mm (in.)	10.6 (0.4)	13.3 (0.5)	11.2 (0.4)	9.9 (0.4)	8.3 (0.3)	10.6 (0.4)
	Failure mode	CC	CC	CC	CC	CC	—
Beam type		N1	N2	N3	N4	N5	—
NSM only	Load, kN (kip)	98.0 (22.0)	94.2 (21.2)	99.9 (22.5)	100.6 (22.6)	101.7 (22.9)	98.9 (22.2)
	Deflection, mm (in.)	9.3 (0.4)	7.8 (0.3)	10.4 (0.4)	11.2 (0.4)	10.8 (0.4)	9.9 (0.4)
	Failure mode	DB	DB	DB	DB	DB	—
Beam type		NU1	NU2	NU3	NU4	NU5	—
NSM + U-wrap	Load, kN (kip)	120.8 (27.2)	118.1 (26.5)	119.6 (26.9)	115.2 (25.9)	121.8 (27.4)	119.1 (26.8)
	Deflection, mm (in.)	12.6 (0.5)	12.2 (0.5)	17.4 (0.7)	15.6 (0.6)	13.3 (0.5)	14.2 (0.6)
	Failure mode	R	R	R	R	R	—
Beam type		NUS1	NUS2	NUS3	NUS4	NUS5	—
NSM + U-wrap shear area	Load, kN (kip)	117.4 (26.4)	107.8 (24.2)	111.6 (25.1)	110.6 (24.9)	NA	111.8 (25.1)
	Deflection, mm (in.)	18.8 (0.7)	12.0 (0.5)	19.0 (0.7)	17.1 (0.7)	NA	16.7 (0.7)
	Failure mode	SE	SE	R	SE	NA	—

Notes: CC is concrete crushing after yielding of steel; DB is debonding of NSM-FRP bar with surrounding epoxy; R is strength rupture of GFRP bar; SE is splitting of epoxy cover.

strengthening. However, it also changes the mode of failure and results in an abrupt failure and a sudden loss of capacity compared with NSM-FRP flexural strengthening. A summary of the change in the load-carrying capacity of the five groups of beams is shown in Fig. 5. A statistical T-test of significance using a 95% level of confidence shows all the beam groups are significantly different compared with control group “C”. The statistical analysis also shows that combining U-wrap with NSM-FRP strengthening resulted in statistically significant results compared with the NSM-FRP strengthening group.

Figure 6 shows the failure mode of all the beam groups and illustrates significant debonding in NSM-FRP and the sudden rupture of GFRP when NSM-FRP is combined with U-wrap shear strengthening. The control groups “C” and “U” have very similar behaviors to conventional RC beams. These two beam series failed in crushing of the concrete after the yielding of steel. Group “N” with NSM-FRP observed debonding of GFRP bar from the surrounding epoxy at 60%

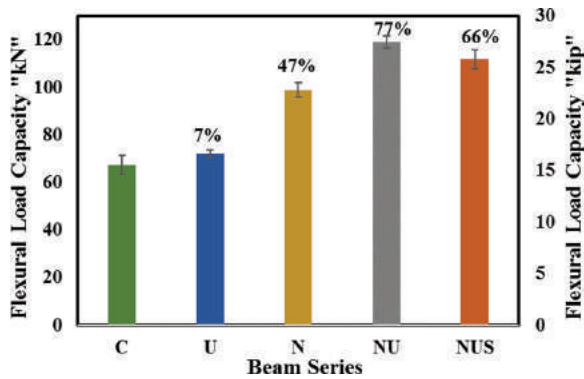


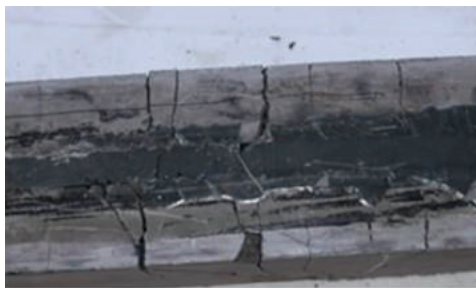
Fig. 5—Mean flexural load capacity of RC beam groups. Percentage represents difference compared with mean flexural capacity of Control ‘C’ RC beam.

of its ultimate strain capacity of the bar along with epoxy cracks, as shown in Fig. 6(a). Group “NU” of RC beams showed significant improvement in bond and changed the mode of failure to rupture of GFRP bar as shown in Fig. 6(b). For group “NUS”, two modes of failure were observed, sudden failure by the sudden splitting of epoxy cover as shown in Fig. 6(c), or GFRP bar rupture as shown in Fig. 6(d). The observed strain in GFRP bar at failure for NUS specimens is 0.0158, which is 88% of the ultimate bar capacity as presented in Table 3. This beam failed with sudden splitting of epoxy cover. It is apparent that the U-wrap confinement enables the GFRP bars not to debond and to reach high strains close to its rupture strain. Two failure modes can then take place, either splitting of the epoxy cover or GFRP bar rupture. If a good epoxy cover is capable of transferring the strain, GFRP rupture would be observed. Otherwise, epoxy cover splitting will be observed.

The experimental program showed that in the “N group”, the GFRP bar starts to slip at the peak load due to debonding of GFRP bar from surrounding epoxy. However, no slip is observed when GFRP U-wrap is used along the full span in the group “NU”. When partial U-wrap is used in the shear

Table 3—Strains in RC beams at failure

Beam	C	U	N	NU	NUS
Strain in concrete top fibers	-0.0036	-0.0035	-0.0024	-0.0026	-0.0029
Strain in steel tension	0.0169	0.0196	0.0133	0.0082	0.0136
Strain in NSM GFRP	NA	NA	0.0100	0.0135	0.0158
Percentage increase in strain capacity in GFRP compared with N RC beam series				35	58



(a)



(b)



(c)



(d)

Fig. 6—Failure modes of RC beams strengthened using FRP: (a) RC-beams series N, failure caused by debonding of NSM-FRP bar; (b) RC-beams series NU, failure caused by tension rupture of GFRP bar; (c) RC-beams series NUS, failure caused by sudden splitting of epoxy cover; and (d) RC-beams series NUS, failure caused by tension rupture of GFRP bar.

span only, slip is observed after the epoxy cover was separated. The absence of end slip associated with U-wrap is shown in Fig. 7. The inset in Fig. 7 shows the displacement of the end plate when slip takes place with NSM-FRP, and the absence of end slip for the case of combining U-wrap with NSM-FRP.

For the control beam group “C”, the strain in tension steel reached 0.0021 yield strain at a load of 44.4 kN (10 kip) and the corresponding midspan deflection measured 3.7 mm (0.14 in.) for Beam C2. The strain gauge stopped reading at a strain of 0.015 and the corresponding load to this strain is 62.9 kN (14.1 kip). At this same point of steel maximum strain, the strain in the top compression fibers reached 0.003 and increased up to 0.0042 and the beam failed due to concrete crushing. The load corresponding to strain 0.0042 recorded at 62.9 kN (14.14 kip) and the corresponding midspan deflection is 10.1 mm (0.4 in.). For beam group “N”, the strain in tension steel reached 0.0021, and the corresponding strain in GFRP bar is 0.0028 with a load measurement of 50.3 kN (11.3 kip) and midspan deflection of 3.4 mm (0.13 in.). The maximum-recorded strain in tension steel was 0.03 at a load of 74 kN (16.6 kip), and the beam failed at a load of 98 kN (22 kip) with the strain in steel measurement of 0.0102. The maximum-recorded strain in concrete compression was 0.0024, and the corresponding load is 98 kN (22 kip). The maximum-recorded strain in the GFRP bar is 0.010, which is 60% of the ultimate strain capacity of the bar. The level of tension in the NSM-GFRP bars is in agreement with that published in the literature.⁷

For the beam group “NU”, the strain in tension steel reached 0.0021; the corresponding strain in GFRP bar is 0.0034, with a load measurement of 73.4 kN (16.5 kip) and midspan deflection of 5.1 mm (0.2 in.). The maximum-recorded strain in tension steel was 0.016 at a load of 108 kN (24.3 kip) and the beam failed at a load of 115.2 kN (25.9 kip) with the strain in steel measurement of 0.0082. GFRP bar rupture caused an abrupt failure and sudden loss of strength. The maximum-recorded strain in the GFRP bar is 0.014, which represents approximately 80% of the ultimate strain capacity of the bar. However, GFRP bar rupture proves that the bar reached its ultimate strain capacity. For beam group “NUS”, the strain in tension steel reached 0.0021, the corresponding strain in GFRP bar is 0.0034, and load measurement of 51.3 kN (11.5 kip) with a corresponding midspan deflection of 3.86 mm (0.15 in.). The maximum-recorded strain in tension steel was 0.014 at a load of 106.4 kN (23.9 kip); however, the beam failed at a load of 111.6 kN (25.1 kip). The strain in steel at failure reached 0.0082. The maximum-recorded strain in concrete compression was 0.0029 and the corresponding load is 105.2 kN (23.6 kip). The maximum-recorded strain in the GFRP bar was 0.018, which is beyond the ultimate strain capacity of the bar. This measurement is attributed to bar debonding followed by sudden splitting of epoxy cover. It is important to note that only one of the four beams in the “NUS” group, failed in GFRP bar rupture. Figure 8 depicts all the aforementioned changes in strains in all the beam groups. It is evident that the continuous U-wrap over the full span confined the

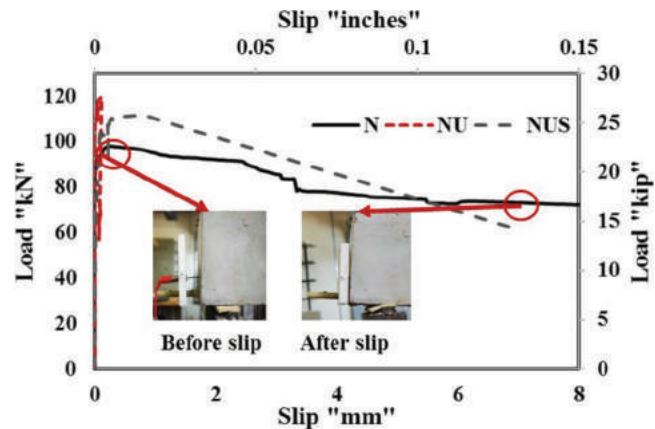


Fig. 7—NSM GFRP bar end slip for N and NUS specimens showing slip to take place with NSM and when U-wrap was used in the shear span only.

NSM-FRP enabling it to reach the ultimate rupture strain. This mode of failure of GFRP rupture is also possible when partial U-wrap in the shear span is used. However, there is higher chance for abrupt epoxy cover splitting prior to GFRP bar rupture in this case. It is important to note the strain distribution at failure is depicted in Fig. 8. The strain distribution for group “N” and “NUS” are nonlinear. This is attributed to debonding of NSM-FRP bars in both cases. Nevertheless, the linear strain distribution in the case of group “NU” shows that no-debonding/slip took place, and the NSM-FRP bar continued to carry the load until rupture.

While the aforementioned testing and analysis make it apparent that combining NSM and U-wrap FRP resulted in changing the failure mode of NSM-FRP strengthened RC beam to a sudden abrupt failure, it is important to quantify the significance of U-wrap on the deformability of RC beams strengthened with NSM-FRP prior to failure. The moment curvatures of all the beam series are presented in Fig. 9. Few methods were borrowed from the previous research to examine the deformability of all the beams.^{16,17,19} The results from the deformability models are presented in a bar plot in Fig. 10. All the results are normalized to their control to enable comparison of the different indexes.

Naaman and Jeongs’s energy-based mode¹⁶ showed a 54% increase in the ductility index for “U”-wrapped RC beams when compared to control RC beams. The RC beams strengthened for flexure using the NSM-FRP technique only “N” showed a decrease in ductility by 59%. RC beams with combined strengthening “NU” showed a slight decrease in ductility by 26% and the combined strengthened RC beams with partial wrap “NUS” showed a decrease in ductility by 43% when compared to the control RC beams “C”.

Jaeger’s moment and deformation-based model¹⁷ showed a 31% increase in the ductility index for “U”-wrapped RC beams when compared to control RC beams. The RC beams strengthened for flexure using NSM-FRP technique only showed a decrease by 20%, combined strengthened RC beams “NU” showed an increase in ductility by 17% and the combined strengthened RC beams with partial wrap “NUS” showed an increase in ductility by 12% when compared to the control RC beams “C”.

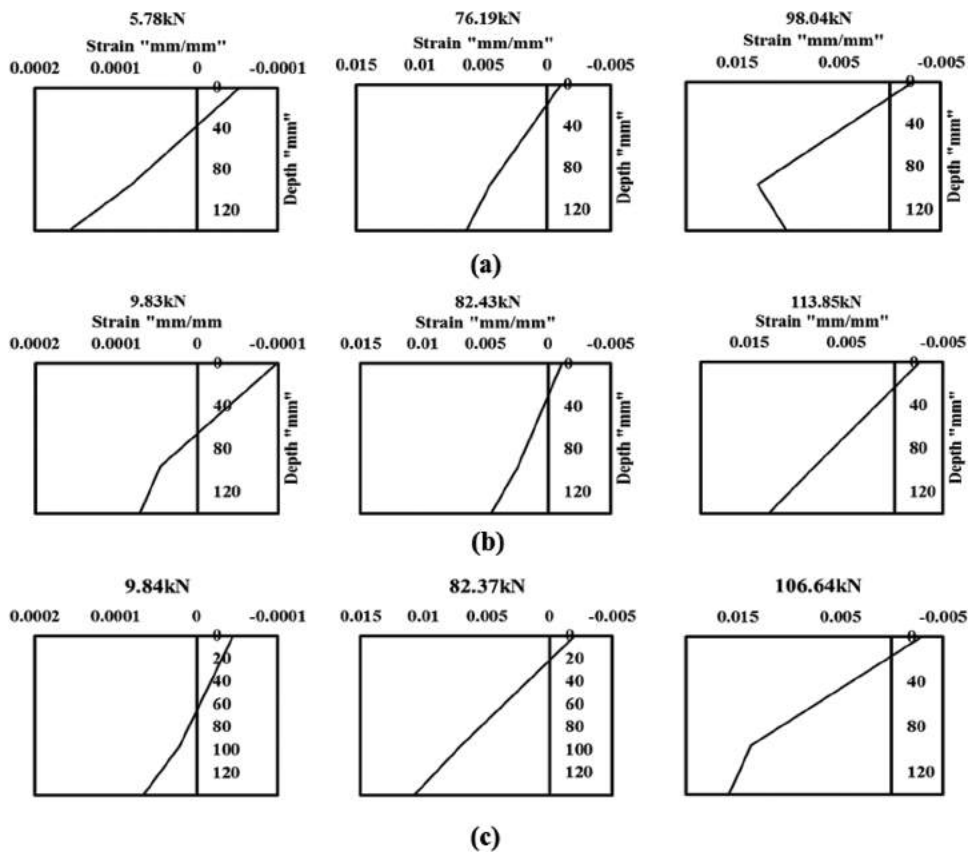


Fig. 8—Strain distribution diagrams at different load levels: (a) RC-beams series N, flexural strengthened using NSM-FRP; (b) RC-beams series NU, flexural strengthened with NSM-FRP technique and shear strengthened using U-wrap FRP wet layup technique; and (c) RC-beams series NUS, flexural strengthened with NSM-FRP technique and shear strengthened using U-wrap FRP wet layup technique. (Note: 1 mm = 0.0394 in.)

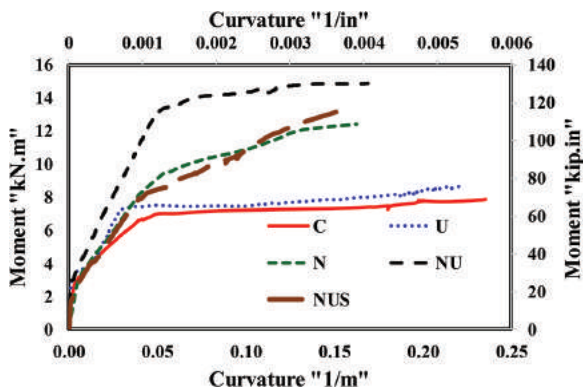


Fig. 9—Moment curvatures of all beam series.

The Abdelrahman et al. deflection-based model¹⁹ showed a 9% decrease in the ductility index for “U” RC beams when compared to control RC beams. The RC beams strengthened for flexure using NSM-FRP technique only showed a ductility index decrease by 29%, combined strengthened RC beams “NU” showed a decrease in ductility index by 1% and the combined strengthened RC beams with partial wrap “NUS” showed an increase in ductility index by 14% when compared to the control RC beams “C”.

The aforementioned analysis shows an obvious trend showing the RC beams strengthened using U-wrap to have a significantly improved ductility. This meets observations

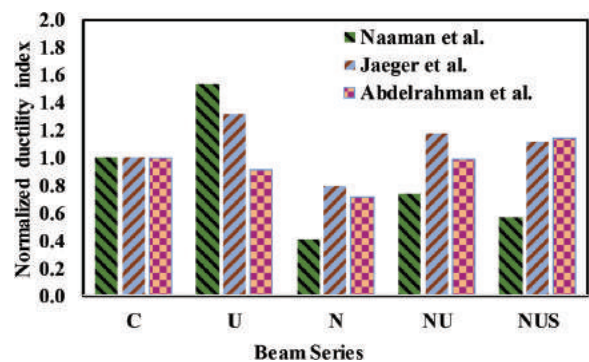


Fig. 10—Ductility index for all five RC beam categories normalized with respect to control RC beam specimens ‘C’.

reported by other researchers for the positive effect of U-wrap confinement on ductility of RC beams strengthened with FRP.^{14,21} RC beams strengthened with NSM-FRP for flexure only showed a sharp decrease in ductility ranging from 20 to 59% compared with the control RC beams. On the other side, full and partial U-wrap with NSM strengthening showed improved ductility compared to beams strengthened with NSM-FRP only making those beams to have very comparable ductility to the original RC beams.

This aforementioned analysis indicates that combining U-wrap for shear strengthening with NSM-FRP flexural strengthening can improve the bond performance and

improve the deformability prior to failure compared with the beams strengthened with NSM-FRP for flexure only.

The aforementioned experimental investigation shows that combining U-wrap shear strengthening with NSM-FRP flexural strengthening improves bond without compromising the beam deformability prior to failure of the RC beams. However, the mode of failure for the combined strengthened beams can be sudden and abrupt. The aforementioned investigation demonstrates that such combination will improve the load-carrying capacity of the strengthened RC beam at the expense of sudden and abrupt failure and sudden loss of capacity due to tension rupture of FRP. The current ACI 440 guidelines for FRP strengthening of RC structures¹¹ do not indicate any potential issue associated with such combination. Further work is needed to ensure designers are aware of such a possibility when the two commonly used strengthening techniques are combined and to limit that effect. One potential solution might be to limit the strain in FRP bars below current design limits suggested by ACI 440 guidelines, when U-wrap shear strengthening is combined with NSM-FRP. Currently, ACI 440¹¹ suggests that the strain in NSM FRP shall not exceed 70% of the ultimate strain capacity. The aforementioned investigation shows that combining U-wrap with NSM FRP strengthening provides confinement that allows the strain in NSM FRP to grow to failure strain causing FRP rupture. The observed increase in FRP strain at failure when U-wrap was used was approximately 40% of the design FRP strain at failure (design strain at failure was 0.010 and recorded failure strain was 0.014). To avoid FRP rupture, with its potential abrupt failure and sudden loss of load-carrying capacity, it is recommended that when NSM is combined with U-wrap strengthening, the strain at failure in NSM FRP shall not exceed 40 to 50% of its ultimate strain capacity. Such a provision will eliminate the possibility of reaching the abrupt failure. Finally, it is interesting to note that the aforementioned investigation suggests that U-wrap in the shear span will provide improved FRP bond without leading to sudden failure. Such improvement in bond in the shear span is necessary to limit fatigue problems in NSM-FRP reported by many researchers.²² Further research is warranted to identify the significance of U-wrap FRP on fatigue performance of NSM-FRP flexural strengthening.

CONCLUSIONS

Experimental observations show that combining U-wrap shear strengthening and NSM-FRP flexural strengthening might result in a significant increase of approximately 77% in the overall flexural capacity compared with control RC beam members and 20% compared with NSM-FRP-strengthened RC beams. However, this increase is associated with abrupt failure, sudden loss of load-carrying capacity. The sudden failure takes place as a result of tension rupture of the NSM-FRP. While NSM-FRP beams showed typical bond slip as reported by many researchers, combining NSM-FRP with U-wrap shear strengthening prevented end slip of GFRP bar and improved the bond strength of NSM-FRP such that the bar continued to carry load up to rupture. Based on the strain data of the NSM-GFRP bar, a 35% increase

was observed for the NU beam series over N beam series showing the improvement in bond between the NSM-FRP bar and surrounding epoxy as a result of U-wraps. However, analysis has also shown an improvement in the deformability for the combined strengthened RC beams when compared to RC beams strengthened for flexure only using NSM-FRP. The aforementioned investigations show the need for imposing limits in ACI guidelines combining the two commonly used strengthening techniques to limit strain in NSM-FRP to 40 to 50% of the ultimate strain capacity to prevent tension rupture or at least make the designers aware of such potential change in the mode of failure and load-carrying capacity when the two strengthening techniques are combined. The aforementioned experimental study also indicates that U-wrap shear strengthening in the shear span might be useful to improve bond and thus eliminate fatigue limitations of NSM-FRP. Further research is warranted to examine the effect of U-wrap on fatigue performance of NSM-FRP strengthened RC-beams.

AUTHOR BIOS

ACI member **Rahulreddy Chennareddy** is a Graduate Student currently pursuing his PhD in the Department of Civil Engineering at the University of New Mexico, Albuquerque, NM. He received his BE from Osmania University, Hyderabad, India, and his MS from the University of New Mexico. His research interests include structural design and rehabilitation using composite and polymer nanocomposite materials in civil engineering.

Mahmoud M. Reda Taha, FACI, is a Professor & Chair of the Department of Civil Engineering at the University of New Mexico. He received BSc and MSc from Ain Shams University, Cairo, Egypt, and his PhD from the University of Calgary, Calgary, AB, Canada. He is Chair of ACI Committee 548, Polymers and Adhesives for Concrete, and a member of ACI Committees 209, Creep and Shrinkage in Concrete; 236, Material Science of Concrete; 241, Nanotechnology of Concrete; 435, Deflection of Concrete Building Structures; and 440, Fiber-Reinforced Polymer Reinforcement. His research interests include structural health monitoring, nanotechnology for structural composites, and structural resilience.

ACKNOWLEDGMENTS

The authors express thanks to K. Martinez and M. Genedy for their continuous help in preparing and testing the specimens. Materials donated by Fyfe Co., LLC, and Euclid Chemicals are greatly appreciated.

REFERENCES

1. Hermann, A. W., "American's Infrastructure: 2013 Report Card," *IABSE Symposium Report*, V. 99, No. 33, *International Association for Bridge and Structural Engineering*, 2013.
2. Huang, R. Y.; Mao, I.; and Lee, H. K., "Exploring the Deterioration Factors of RC Bridge Decks: A Rough Set Approach," *Computer-Aided Civil and Infrastructure Engineering*, V. 25, No. 7, 2010, pp. 517-529. doi: 10.1111/j.1467-8667.2010.00665.x
3. Bakis, C.; Bank, L. C.; Brown, V.; Cosenza, E.; Davalos, J.; Lesko, J.; Machida, A.; Rizkalla, S. H.; and Triantafyllou, T. C., "Fiber-Reinforced Polymer Composites for Construction-State-of-the-Art Review," *Journal of Composites for Construction*, ASCE, V. 6, No. 2, 2002, pp. 73-87. doi: 10.1061/(ASCE)1090-0268(2002)6:2(73)
4. Saadatmanesh, H., and Ehsani, M., "Fiber Composite Plates Can Strengthen Beams," *Concrete International*, V. 12, No. 3, Mar. 1990, pp. 65-71.
5. Nanni, A.; Alkhrdaji, T.; Barker, M.; Chen, G.; Mayo, R.; and Yang, X., "Overview of Testing to Failure Program of a Highway Bridge Strengthened with FRP Composites," *Proceedings of the 4th International Symposium on Non-Metallic (FRP) Reinforcement for Concrete Structures (FRPRCS-4)*, Baltimore, MD, 1999, pp. 69-75.
6. De Lorenzis, L., and Teng, J., "Near-Surface Mounted FRP Reinforcement: An Emerging Technique for Strengthening Structures," *Composites. Part B, Engineering*, V. 38, No. 2, 2007, pp. 119-143. doi: 10.1016/j.compositesb.2006.08.003
7. Hassan, T. K., and Rizkalla, S. H., "Bond Mechanism of Near-Surface-Mounted Fiber-Reinforced Polymer Bars for Flexural Strength-

ening of Concrete Structures,” *ACI Structural Journal*, V. 101, No. 6, Nov.-Dec. 2004, pp. 830-839.

8. Yan, X.; Miller, B.; Nanni, A.; and Bakis, C., “Characterization of CFRP Rods Used as Near Surface Mounted Reinforcement,” 8th International Conference on Structural Faults and Repair, Edinburgh, Scotland, 1999.

9. De Lorenzis, L.; Lundgren, K.; and Rizzo, A., “Anchorage Length of Near-Surface Mounted Fiber-Reinforced Polymer Bars for Concrete Strengthening-Experimental Investigation and Numerical Modeling,” *ACI Structural Journal*, V. 101, No. 2, Feb.-Mar. 2004, pp. 375-386.

10. Lorenzis, L. D., and Nanni, A., “Characterization of FRP Rods as Near-Surface Mounted Reinforcement,” *Journal of Composites for Construction*, V. 5, No. 2, 2001, pp. 114-121. doi: 10.1061/(ASCE)1090-0268(2001)5:2(114)

11. ACI Committee 440, “Guide for the Design and Construction of Externally Bonded FRP Systems for Strengthening Concrete Structures (ACI 440.2R-08),” American Concrete Institute, Farmington Hills, MI, 2008, 76 pp.

12. Chajes, M. J.; Januszka, T. F.; Mertz, D. R.; Thomson, T. A. Jr.; and Finch, W. W. Jr., “Shear Strengthening of Reinforced Concrete Beams Using Externally Applied Composite Fabrics,” *ACI Structural Journal*, V. 92, No. 3, May-June 1995, pp. 295-303.

13. Malvar, L.; Warren, G.; and Inaba, C., “Rehabilitation of Navy Pier Beams with Composite Sheets,” *RILEM Proceedings*, Chapman and Hall, 1995, pp. 533-540.

14. Kachlakev, D., and McCurry, D., “Behavior of Full-Scale Reinforced Concrete Beams Retrofitted for Shear and Flexural with FRP Laminates,” *Composites. Part B, Engineering*, V. 31, No. 6, 2000, pp. 445-452. doi: 10.1016/S1359-8368(00)00023-8

15. Augustine, F. W., “Strengthening Rectangular Beams with NSM Steel Bars and Externally Bonded GFRP,” master’s thesis, Kansas State University, Manhattan, KS, 2013.

16. Naaman, A., and Jeong, S. M., “Structural Ductility of Concrete Beams Prestressed with FRP Tendons. In Non-Metric (FRP) Reinforcement for Concrete Structures,” *Proceedings of the 2nd International RILEM Symposium (FRPRCS-2)*, Ghent, Belgium, Aug. 23-25 1995, pp. 379-386.

17. Jaeger, L.; Mufti, A.; and Tadros, G., “The Concept of the Overall Performance Factor in Rectangular-Section Reinforced Concrete Members,” *Proceedings of the 3rd International Symposium on Non-Metallic (FRP) Reinforcement for Concrete Structures*, Sapporo, Japan, 1997, pp. 551-559.

18. Zou, P. X. W., “Flexural Behavior and Deformability of Fiber Reinforced Polymer Prestressed Concrete Beams,” *Journal of Composites for Construction*, V. 7, No. 4, 2003, pp. 275-284. doi: 10.1061/(ASCE)1090-0268(2003)7:4(275)

19. Abdelrahman, A. A.; Tadros, G.; and Rizkalla, S. H., “Test Model for First Canadian Smart Highway Bridge,” *ACI Structural Journal*, V. 92, No. 4, July-Aug. 1995, pp. 451-458.

20. Dongkeun, L.; Lijuan, C.; and Jason Yan-Gee, H., “Bond Characteristics of Various NSM FRP Reinforcements in Concrete,” *Journal of Composites for Construction*, V. 17, No. 1, 2012, pp. 117-129.

21. Kotynia, R., “Debonding Failures of RC Beams Strengthened with Externally Bonded Strips,” *Proceedings of the International Symposium on Bond Behaviour of FRP in Structures (BBFS 2005)*, 2005.

22. Chen, C., and Cheng, L., “Fatigue Bond Characteristics and Degradation of Near-Surface Mounted CFRP Rods and Strips in Concrete,” *Journal of Composites for Construction*, ASCE, V. 18, No. 2, 2015